Catalysis Today 165 (2011) 112–119

Contents lists available at ScienceDirect

Catalysis Today

journal homepage: www.elsevier.com/locate/cattod

Theoretical studies of Na^+ location in ZSM-5: Model selection for accurate coordination structure and energetics

Zhen-Kun Chu [a], Gang Fu [a], Xin Xu [a,b,*]

[a] State Key Laboratory of Physical Chemistry of Solid Surfaces, College of Chemistry and Chemical Engineering, Xiamen University, Xiamen 361005, China
[b] Shanghai Key Laboratory of Molecular Catalysis and Innovative Materials, MOE Key Laboratory for Computational Physical Science, Department of Chemistry, Fudan University, Shanghai 200433, China

ARTICLE INFO

Article history:
Received 16 August 2010
Received in revised form
13 December 2010
Accepted 17 December 2010
Available online 31 January 2011

Keywords:
Zeolite
Cation location
Cluster model

ABSTRACT

Location of Na^+ in ZSM-5 zeolite has been studied with cluster models and density functional theory of B3LYP. Various cluster models with sizes ranging from 3T to 192T were employed. Their performance in geometry optimization and stability assessment of four probable Na-sites at **T1**, namely Z6, M7, I2 and I3, were systematically studied. A C-5 type model is constructed by allowing all atoms on the three rings around the Al site to relax during the geometry optimization, and then expanding the region by roughly another three shells of Si atoms, leading to converged prediction of stability sequence of Z6 > I2 > M7 > I3. Based on these results, a general scheme of cluster model construction for reliable prediction of metal cation location in zeolite is proposed.

1. Introduction

Metal cation exchanged zeolites have attracted great industrial and academic interests due to their excellent catalytic properties [1–3]. Metal cation compensates the negative charge in the zeolite framework resulting from Si–Al substitution (see Fig. 1 for a schematic representation). These charge-compensating cations could act as Lewis acid sites or redox active centers or both during a catalytic process [2]. Various possible location sites are available for metal cations, as most zeolites have complex channel and cavity structures. Cations on these sites may coordinate to different numbers of framework oxygen atoms, giving different electronic structures of the cation sites, which show rather different levels for HOMO (highest occupied molecular orbitals) and LUMO (lowest unoccupied molecular orbitals), resulting in different ability of donating and accepting electrons. Furthermore, metal cations on these sites may have different accessibility to reactants. Hence reactions take place on these sites will suffer from different stereo-hindrance, showing uneven shape-selectivity. All these factors will lead to the distinct catalytic activities of different cation location sites [1,4]. Finding out the preferred location sites for extra-framework cations is a vital step for catalytically active center characterization and finally the reaction mechanism elucidation at the molecular level.

Lots of experimental efforts have been devoted to the location of extra-framework cations in zeolite. Besides modern crystallographic techniques [5,6], various methods, particularly UV–vis [7–12], FTIR [10–16], microcalorimetry [14–16], NMR [17], ESR [18–21], and EXAFS [20–24] have been used to serve this purpose. However, limitations of a specific experimental method are also well recognized. As the concentration of the extra-framework cations in high-silica zeolites is low, the distribution of the cations may not be uniform in different unit cells, such that the location of extra-framework cations may lack real periodicity. In this case, the interpretation of the electron density map from the X-ray diffraction method can be difficult and even ambiguous [5,6]. Many studies used small probe molecules (e.g., CO, N_2 and CH_3OH) and various spectral methods (e.g., FTIR and NMR) to investigate the cation location in various alkali-exchanged ZSM-5 zeolite [13–17]. Some useful information has been obtained, such as the number of the kinds of location sites and their accessibility to small molecules in the gas phase. But unambiguous location and accurate coordination structure of those cations are not available by these types of methods.

Computational methods provide a useful tool, which complements the experimental methods to study the coordination structures for cations on different location sites as well as the relative stability of these sites. For example, Vayssilov et al. [25] studied Na^+ location on the so-called **SII** site in the FAU zeolite and used

* Corresponding author at: Shanghai Key Laboratory of Molecular Catalysis and Innovative Materials, MOE Key Laboratory for Computational Physical Science, Department of Chemistry, Fudan University, Handan Lu 220, Shanghai 200433, China.
E-mail addresses: xxchem@fudan.edu.cn, xinxu@xmu.edu.cn (X. Xu).

0920-5861/$ – see front matter © 2011 Elsevier B.V. All rights reserved.
doi:10.1016/j.cattod.2010.12.043

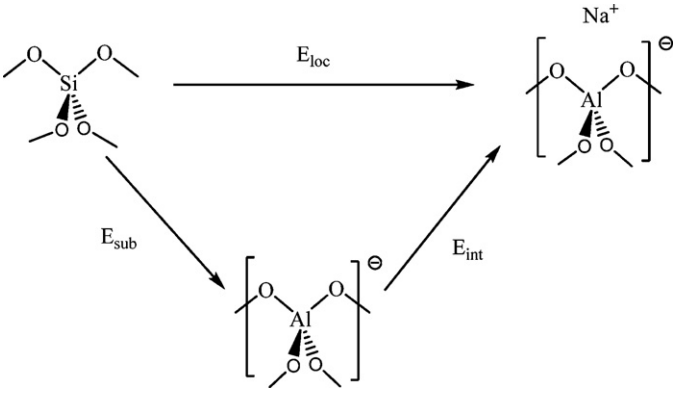

Fig. 1. Schematic representation of extra-framework cation location associated with Al substitution in a given tetrahedral site.

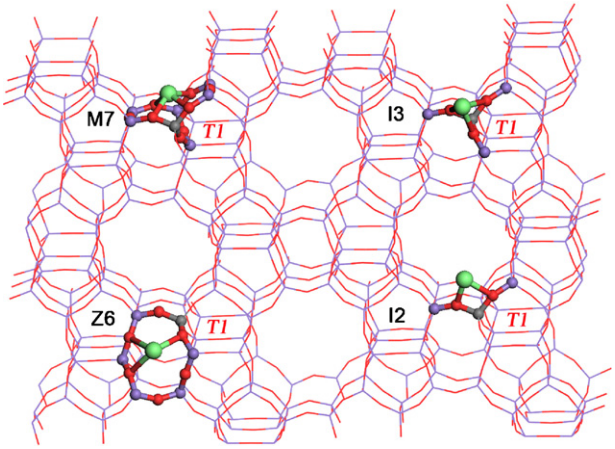

Fig. 2. Four probable Na-sites associated with Al substituted **T1** site.

6T (T stands for tetrahedron of [SiO_4] or [AlO_4]) cluster models to represent the six-member ring on the channel wall. Rice et al. [26] used 4T–6T small clusters to model the cation sites on top of four-, five-, six-member rings for a series of divalent cations in the ZSM-5 zeolite. By comparing the calculated binding energies of the cation at different sites, the preferred locating positions were predicted. Nachtigallova et al. [27] used a combined quantum mechanics/interatomic potential function method (QM-pot) to study the preferred coordination site of Cu^+ in several **T**-sites in ZSM-5. The QM parts (4T–6T) used in their work [27] were similar to those cluster models used by Rice et al. [26] The same computational scheme was used by Kucera and Nachtigall [28] to study Li^+, Na^+, K^+ location in ZSM-5. Periodic DFT methods were also used to investigate the location of extra-framework species [29–31]. But due to the sharply increased computation expense with increasing unit cell size, periodic DFT studies were mainly limited to zeolites with relatively small unit cells (e.g., CHA).

On the other hand, it is also well known that the reliability of the results by cluster models largely depends on the model selection [32,33]. This is also a key issue in setting up hybrid models consisting of a cut-out cluster model as the high-layer [27,32–38]. From a point of view of computational efficiency, small cluster models are preferred. However, for studies of cation locations in zeolites, small clusters consisting of only several [SiO_4]/[AlO_4] tetrahedrals may suffer from serious errors. Firstly, to maintain the framework structures of zeolites, partial geometry optimization is usually carried out. This can impose too much constraint on the cation sites, resulting in erroneous coordination structures. Secondly, to set up a cluster model, one has to cut out the model system from the framework of zeolite. The perturbation on the wave functions of the active centers by cutting off the Si–O bonds and terminating the dangling bonds with H atoms can be rather serious for such small clusters. This also contributes to the boundary effects in some hybrid methods such as 'our own n-layered integrated molecular orbital and molecular mechanics' ONIOM method [34–37]. Finally, the long-range interaction which is especially important for such cationic systems is totally absent in bare small cluster calculations. To the best of our knowledge, however, there is no systematic investigation of cluster model selection for cation locations in zeolites.

Alkali cations (particularly Na^+) often act as the compensating ion when zeolite is firstly synthesized [39]. In the alkali-form zeolites, alkali cations act as the Lewis acid site, while the oxygen atoms in the [AlO_4] tetrahedron serve as the basic site. Such acid–base pairs are believed to be closely associated with the catalytic properties of the alkali-form zeolites [40–43]. ZSM-5 is a representative high-silica zeolite and is industrially very important [44]. Here we present a systematic study of cluster model selection for Na^+ location in ZSM-5 as an instructive example for metal cation locations in zeolites.

A series of cluster models with sizes ranging from 3T to 192T were constructed and their performance in coordination structure optimization and stability sequence prediction of different sites were tested. Converged coordination structure and stability sequence were obtained, such that a general scheme of cluster model construction for reliable prediction of metal cation locations in zeolites was proposed.

2. Models and computational methods

ZSM-5 zeolite typically crystallizes in orthorhombic space group ***Pnma***, and twelve crystallographically distinct **T**-sites exist in its framework [45]. Among them, **T1** was predicted to be one of the most stable Al substitution sites [27] and has been used as the Al substitution site in other theoretical studies [46]. Once Si–Al substitution occurs at **T1**, we found four probable sites for Na^+: Z6, M7, I2 and I3 (see Fig. 2). Symbol Z6 denotes the cation site on top of the six-member ring in the zigzag channel. Similarly, M7 represents the site on top of the six-member ring in the main channel with an additional [SiO_4] at the bottom of the ring. I2 and I3 denote the sites located at the intersection of the main and zigzag channels, at which Na^+ is coordinated to two or three oxygen atoms of [AlO_4], respectively. For each site, cluster models with increasing sizes (3T–192T) were constructed. Their performance in coordination structure optimization and stability sequence prediction were tested.

To assess the relative stability of different Na^+ locations for a given **T** site, interaction energy (E_{int} for short, see Fig. 1) between Na^+ and the zeolite framework may be defined. For example, E_{int} of the M7 site is expressed as:

$$E_{int}(M7) = E_{Al^-\text{–}Na^+}(M7) - \left[E_{Al^-}(M7) + E_{Na^+}\right] \quad (1)$$

here the subscript Al^- represents the cluster model with Si atom at **T1** substituted by Al. Note that it carries a negative charge. Al^-–Na^+ represents the cluster with a Na^+ compensating the negative charge of the Al^- cluster. E_{int} defined here is the same as the binding energy used by Rice et al. [26], as well as by Nachtigall et al. [27,28]

Here we introduce another indicator, namely cation location energy (E_{loc} for short, see Fig. 1) to assess the Na-site stability associated with a given **T** site for Al substitution. Hence, E_{loc} of the M7 site is expressed as:

$$E_{loc}(M7) = E_{Al^-\text{–}Na^+}(M7) - E_{Si}(M7) \quad (2)$$

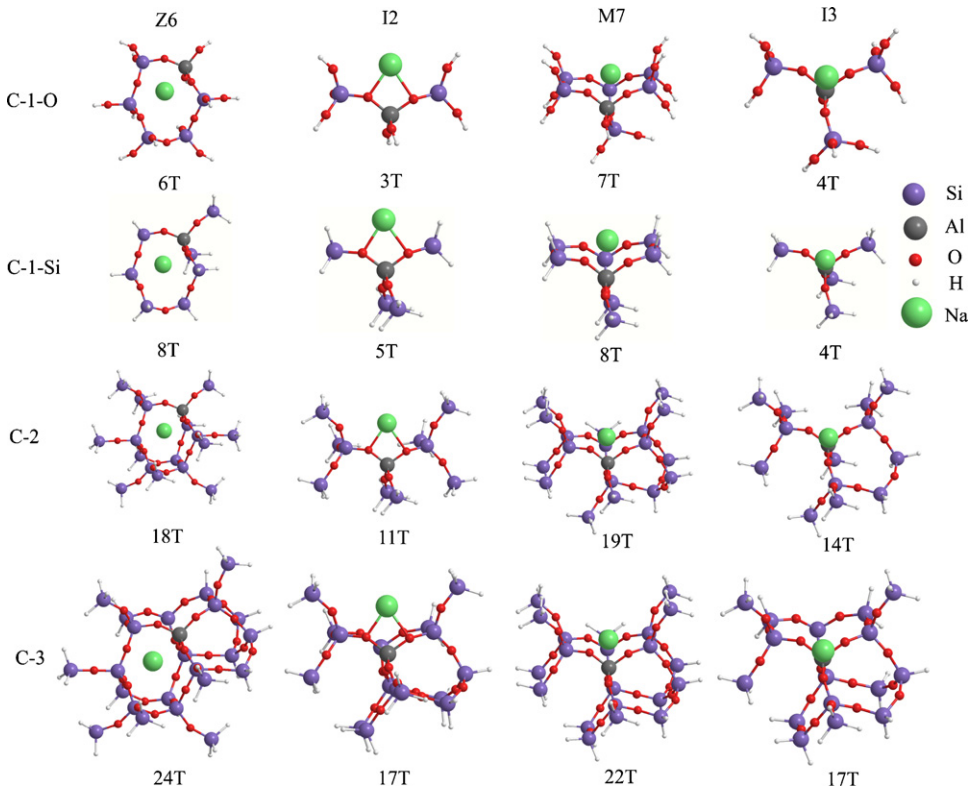

Fig. 3. C-1-O, C-1-Si, C-2 and C-3 cluster models for all four Na-sites.

where the subscript Si represents a siliceous cluster before Si–Al substitution. Note that the negatively charged Al^- cluster is not directly involved in such a definition, which may show less basis set dependence.

In Fig. 1, we also define E_{sub} for the energy change due to Si–Al substitution at a given **T** site. In the literature, the term 'substitute energy' may be defined based on the substitution of Si(IV) by a pair of Al(III)$\cdots M^+$ [47,48]. Such a definition is the same as E_{loc} used here. Indeed, it is possible to use E_{loc} to study cation location associated with different **T** site.

To access the relative stability, ΔE_{loc} or ΔE_{int} may be used:(3)$\Delta E_{int}(M7) = \left[E_{Al^-\text{–}Na^+}(M7) - E_{Al^-\text{–}Na^+}(Z6)\right] - \left[E_{Al^-}(M7) - E_{Al^-}(Z6)\right]$

$$\Delta E_{loc}(M7) = \left[E_{Al^-\text{–}Na^+}(M7) - E_{Al^-\text{–}Na^+}(Z6)\right] - [E_{Si}(M7) - E_{Si}(Z6)] \quad (4)$$

here we use the Z6 site as the reference, as it is the most stable Na-site associated with **T1** concluded in this work. Note that the second term in the parenthesis of Eq. (3) or (4) is due to the different choice of cluster model for different site, which is artificial and has to be subtracted from the first term to get the intrinsic relative stability for the Na-sites. Due to different electronic nature of the negatively charged Al^- clusters and neutral Si clusters, it is expected E_{int}, ΔE_{int}, and E_{loc} and ΔE_{loc} show different size dependence for model selection, which is the main theme to be examined in the present work.

A series of cluster models with increasing sizes (3T–192T) were constructed for all four Na-sites: namely C-1-O, C-1-Si, C-2, C-3, C-4, C-5, C-6 and C-7. These cluster models are depicted in Figs. 3 and 4. All of them were cut out from the experimental crystallographic structure of ZSM-5 [45]. The dangling bonds resulting from breaking the Si–O valance bonds were saturated by H atoms. C-1-O used O–H termination and the terminal O–H bond length was fixed at 0.97 Å. All other clusters used Si–H termination with the Si–H bond lengths fixed at 1.47 Å.

These cluster models can be assigned into two categories: **Type I** and **Type II**. Cluster models of **Type I** include C-1-O, C-1-Si, C-2 and C-3. Due to their small sizes, each **Type I** cluster includes only the appropriate coordination environment for one of the four Na-sites. Thus as can be seen in Fig. 3, **Type I** clusters for different Na-sites comprise different parts of the zeolite framework, and have different sizes. On the contrary, clusters of **Type II** are big enough to

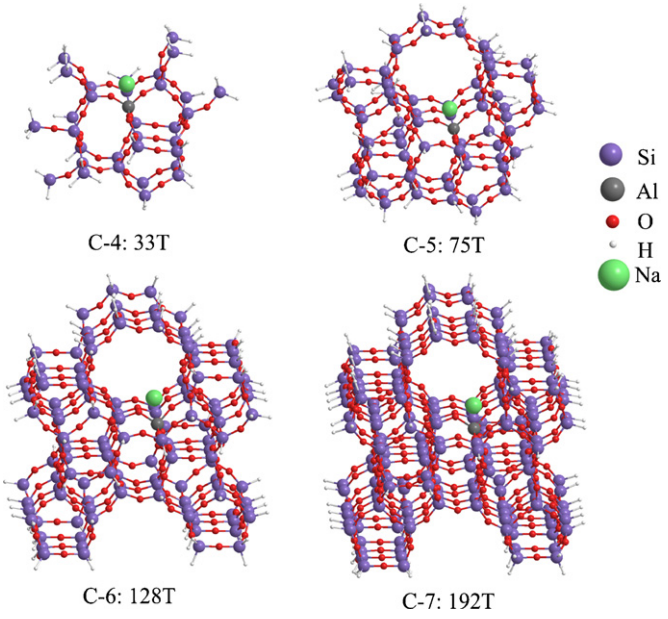

Fig. 4. C-4, C-5, C-6 and C-7 cluster models for the M7 site.

Table 1
The optimized Na–O bond lengths and calculated relative stability (ΔE) of different Na-sites with different basis sets. Calculations are based on C-4:33T models.

Basis set	Na-sites	Na–O bond length (Å)[a]	ΔE (kcal/mol)
3-21G*	Z6	2.150, 2.756, 3.740, 2.253, 2.426, 3.777	0.0
	M7	2.166, 3.014, 2.284, 2.699, 2.241, 2.948	−2.33
	I2	2.138, 2.271	16.75
	I3	2.240, 2.267, 2.224	11.85
6-31G*	Z6	2.204, 3.377, 4.104, 2.410, 2.322, 3.428	0.0
	M7	2.196, 2.450, 3.452, 2.354, 2.478, 3.699	3.21
	I2	2.221, 2.351	5.85
	I3	2.383, 2.456, 2.373	6.45
6-31+G*	Z6	2.209, 3.438, 4.151, 2.421, 2.323, 3.409	0.0
	M7	2.198, 2.482, 3.441, 2.368, 2.505, 3.709	2.66
	I2	2.233, 2.364	4.03
	I3	2.394, 2.506, 2.373	5.33
6-311+G**	Z6	2.212, 3.413, 4.109, 2.419, 2.327, 3.441	0.0
	M7	2.204, 2.461, 3.449, 2.368, 2.501, 3.689	3.43
	I2	2.233, 2.356	4.60
	I3	2.384, 2.453, 2.402	4.89

[a] Na–O bond lengths for Z6 listed here are between the Na^+ and the six O atoms on the Z6 ring: 1-10-11-7-4-5-1 (the numbers denote the T sites connected to the O atoms [45]). For M7: the six O atoms on the M7 ring are 5-1-2-8-7-11-5. For I2: the two O atoms are 5-1-2. For I3: those three O atoms are 5-1-2 and 1-10.

include all four adsorption sites for Na^+ in a single cluster. Fig. 4 shows the model for Na^+ adsorbed on the M7 site, as an example. Models for other Na-sites can be conveniently constructed by putting Na^+ at the appropriate sites as shown in Fig. 2. Hence, four adsorption sites have the same size for cluster models of **Type II**. For cluster models of **Type I**, one has to use either ΔE_{int} or ΔE_{loc} to compare their relative stability for different Na-sites, but for **Type II**, one can directly compare the energy differences between the cluster models (ΔE) for different Na-sites. In such case, ΔE_{int} and ΔE_{loc} given in Eqs. (3) and (4), respectively, are both converted to ΔE as:

$$\Delta E(\mathrm{M7}) = [E_{\mathrm{Al^-\text{–}Na^+}}(\mathrm{M7}) - E_{\mathrm{Al^-\text{–}Na^+}}(\mathrm{Z6})] \quad (5)$$

All the calculations were performed using the three-parameter hybrid density functional B3LYP [49–53]. In order to study the basis set effect, four basis sets namely 3-21G* [54–59], 6-31G* [60–62], 6-31+G* [63,64] and 6-311+G** [65–69] were assessed for their performance both in geometry optimization and single point energy calculation. For clusters no larger than 33T, analytical frequencies were calculated to confirm that all local minima have no imaginary frequency and to get the zero-point vibrational energies. We found that including zero-point vibrational energy changed the results by no larger than 0.3 kcal/mol in the relative stability calculations of different sites. Thus for clusters larger than 33T, frequency calculations were not carried out, due to its too large calculation expense for these huge clusters.

All the calculations were performed using Gaussian 03 package [70].

3. Results and discussions

3.1. Basis set effect

The optimized Na–O bond lengths with C-4:33T clusters for all four Na-sites using B3LYP and four different basis sets, 3-21G*, 6-31G*, 6-31+G* and 6-311+G** are summarized in Table 1. All four basis sets have been used before in the literature to study the related zeolite properties [71–75]. It can be seen that 3-21G* optimized Na–O bond lengths are distinctly different from those by 6-31G*, whereas the Na–O bond lengths by 6-31G* and 6-31+G* are quite similar to those from 6-311+G** with a MAD (Mean absolute deviation) of only 0.011 and 0.016 Å, respectively. By contrast, MAD of the 3-21G* optimized bond lengths with respect to those by 6-311+G** is as high as 0.321 Å. So it can be seen that 6-31G* is a basis set that can provide similar coordination structure to that of 6-311+G** for Na^+ at a relatively low expense.

Table 2
The numbers of the relaxed atoms (N_r) in geometry optimization and the average optimized Al–O bond lengths (L_{Al-O}, Å) in the [AlO_4] tetrahedron for different cluster models[a].

Cluster model	Z6		I2		M7		I3	
	N_r	L_{Al-O}	N_r	L_{Al-O}	N_r	L_{Al-O}	N_r	L_{Al-O}
C-1-O	13	1.681	6	1.682	16	1.708	8	1.703
C-1-Si	17	1.721	10	1.723	18	1.725	10	1.723
C-2	25	1.723	14	1.713	28	1.741	18	1.713
C-3	33	1.732	22	1.725	32	1.737	22	1.726
C-4	50	1.741	50	1.738	50	1.736	50	1.740
C-5	50	1.741	50	1.741	50	1.736	50	1.739
C-6	68	1.742	68	1.740	68	1.737	68	1.739

[a] For Al^-–Na^+ form clusters.

The relative stability of the Na-sites (i.e., ΔE of I2, M7, I3 with respect to Z6) predicted by 3-21G*, 6-31G*, 6-31+G* and 6-311+G** is also summarized in Table 1. It can be seen that M7 is predicted to be the most stable site by 3-21G*, while Z6 is shown to be the most stable one by 6-31G*, 6-31+G* and 6-311+G**. Actually the stability sequences for all four sites by 6-31G*, 6-31+G* are identical to that from 6-311+G**, while 3-21G* presents completely different stability sequence from that by 6-311+G** and shows a clear tendency to underestimate the stability of I2 or I3. For C-4:33T model, 6-31G* reduces the number of basis set from 2262 of 6-311+G** to 1405. In the rest part of this work, all results presented are obtained using the 6-31G* basis set to facilitate calculations of large clusters. For C-7:192T, a total of 636 atoms are involved with 8778 basis functions at 6-31G*.

3.2. Geometry optimization by different cluster models

Acquiring the accurate coordination structure for cations is important for active center characterization in zeolite. In order to reflect the constraint effect of the zeolite lattice on the structure of the active site, partial optimization is usually employed [76]. And the reliability of the results could largely be influenced by the selection of the relaxed part during the partial optimization [77,78]. In the metal cation location studies in zeolite, the Si–Al substitution and subsequent cation adsorption would lead to drastic perturbation on the local structure. So there is a particularly urgent demand for a systematic investigation on the dependence of coordination structure optimization of cation on the cluster model selection. Here we use Na^+ location in ZSM-5 as an example.

As the cluster sizes increase from C-1-O to C-6, the numbers of atoms allowed to relax in the optimization are also increased accordingly (see N_r in Table 2). For example, from C-1-O to C-4 clusters of the Al^-–Na^+ models, the number of atoms relaxed during geometry optimization increases gradually from the smallest 6 (C-1-O for I2 site) to 50. In C-4:33T, besides Na^+ and [AlO_4], all [SiO_4] on the three rings around the Al substituted **T1** site and all four [SiO_4] that directly coordinate to Al, are allowed to relax. In C-5:75T, the same relaxed region as that in C-4 model is adopted in order to investigate the effect of the zeolite environment on the Na-site structure optimization. In C-6:128T, the relaxed region is further enlarged by another shell of Si atoms from that of C-4 and C-5 and the number of relaxed atoms reaches 68.

The average Al–O bond lengths of the [AlO_4] tetrahedron obtained by different cluster models (C-1-O to C-6) are summarized in Table 2. The average Al–O bond length in Na-FAU zeolite found in EXAFS experiment is 1.74 Å (no experimental result for Na-ZSM-5 is available) [79]. It is distinct that for small clusters like C-1-O, the optimized Al–O bond lengths are much shorter than 1.74 Å. With

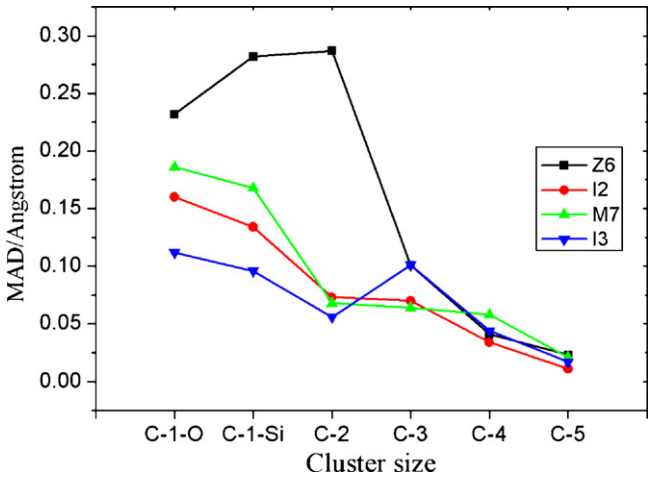

Fig. 5. Dependence of the optimized Na-site coordination structure on cluster size.

the relaxed region enlarged, the Al–O bond lengths increase gradually. When the model size is up to those in C-4, the Al–O bond lengths for all four Na-sites are less than 0.005 Å apart from 1.74 Å. Further increasing the model size or enlarging the relaxed region causes negligible change. So we can conclude that small clusters impose too much constraint on the active site structure that leads to too short Al–O bond lengths. By relaxing all the rings around Al substituted site in C-4 and C-5, the structure of the Na-site is fully relaxed and the average Al–O bond lengths tend to approach to the converged value.

Using results of C-6 as references, we further evaluate MADs of the optimized Na–O bond lengths by cluster models of C-1-O to C-5. The results are displayed in Fig. 5. Due to the serious constraint effects, MAD of the Na–O bond length of C-1-O cluster for Z6 is as large as 0.232 Å. Even for I3, which possesses the smallest errors in the C-1-O models, is still larger than 0.1 Å. As the cluster size and the number of the relaxed atoms increase, the errors for the Na–O bond lengths gradually decrease. With all the three rings around **T1** relaxed during geometry optimization as in the C-4 model, the biggest error is only 0.058 Å, which is about 1/4 of those associated with C-1-O and C-1-Si. So it can be seen that full relaxation of the active region structure is a requisite for reliable prediction of the Na^+ coordination structure.

However, despite the same relaxed regions for C-5 and C-4 clusters, their optimized structures are still rather different. As compared to those of C-4, MADs of the Na–O bond lengths for various C-5 models further decreased dramatically (e.g. the largest for Z6 is 0.023 Å and the lowest for I2 only 0.011 Å). Two reasons should contribute to this improvement: (1) the reduced boundary effect, (2) the better description of the long-range interaction. The Mulliken charges on the Si atoms in the terminal SiH_3 groups of the C-4 clusters are only about +0.5, whereas, in C-5, these Si atoms are no longer in the terminal SiH_3 groups but in the $[SiO_4]$ tetrahedral and the charges on them are now about +1.1. These differences in electronic structure of this boundary area should have significant effects on the optimized Na^+ coordination structure. Even though C-5 has the same relaxed region as C-4, the former incorporates the long-range interaction of the zeolite environment beyond C-4 that should be rather important for this cationic system. Hence, in addition to a fully relaxed structure of the active center, diminishing the boundary effect and including the necessary zeolite environment are also important for reliable coordination structure optimization of metal cations in zeolites.

To further investigate the effect of the difference between the optimized structures by C-4 and C-5, and that between C-5 and C-6, on the relative stability prediction of the Na-sites, the optimized C-4, C-5 structures were embedded into the C-5 and C-6 models, respectively. Then single-point energy calculations were performed on the C-4-embedded-C5 (C-5*, for short) and C-5-embedded-C-6 clusters (C-6*, for short). The results are listed in Table 3 and compared to those of C-5 and C-6. It can be seen that C-5* models induced different stability sequence from C-5. The stability sequence of I2 and M7 was reversed. In contrast, C-6* clusters provided a stability sequence that was exactly the same as that of C-6. Hence, we conclude that coordination structures of Na^+ by C-5 are good enough and further enlarging the relaxed region and the size of the full cluster will cause no significant difference in stability prediction of the Na-sites.

Table 3
ΔE (kcal/mol) of I2, M7 and I3 with respect to Z6 by single point calculation with different models.

Models	I2	M7	I3
C-4-embedded-C5 (C-5*)	5.14	4.62	5.74
C5	2.92	4.48	5.46
C-5-embedded-C6 (C-6*)	2.59	4.21	4.93
C6	2.60	3.69	5.07

3.3. Dependence of E_{int} or E_{loc} on cluster model selection

For clusters of **Type I** (C-1-O to C-3), one may use either E_{int} or E_{loc} to evaluate the relative stability of different sites. Such small cluster model calculations are important, as they present models that are affordable for high level calculations. However, such kind of high level calculations are relevant only when the model systems faithfully represent the real system. Hence it is important to examine the dependence of E_{int} or E_{loc} on cluster model selection. For clusters of **Type II** (C-4 to C-7), examination of size dependence is also important. Even though **Type II** clusters are large enough to accommodate all four Na-sites in a single model, some sites may be better described than the other sites for a specific model. Hence it is important to study how the stability prediction of the Na-sites depends on the cluster model selection for both **Type I** and **Type II** models.

For all the C-1-O to C-7 models, we calculated E_{int} and E_{loc} for all four sites. As C-5 optimized structures were found reliable and the C-5-embedded-C-6 (C-6*) model led to the same trend as that of C-6, we used C5-embedded-C7 (C-7*) for single point energy calculations to avoid further optimization of the huge C-7:192T clusters and assess the effect of the long-range interactions beyond C-5 clusters.

Table 4 displays E_{int} calculated with different cluster models. As it can be seen, E_{int} changes intensively with the increasing cluster size. C-1-O clusters overestimate E_{int} by about 50 kcal/mol, as compared to the results by the largest C-7 clusters. And E_{int} decreases sharply by more than 30 kcal/mol from C-1-O to C-1-Si. By increasing the cluster sizes from C-1-Si to C-7, the calculated E_{int} decrease gradually and are not convergent even at the C-7 model consisting of 192T. Brand et al. [80] has compared the performance of

Table 4
Dependence of E_{int} on cluster model selection (kcal/mol).

Cluster size	Z6	I2	M7	I3
C-1-O	−167.65	−162.46	−161.48	−160.87
C-1-Si	−127.12	−126.54	−125.13	−127.63
C-2	−126.90	−124.80	−126.22	−120.65
C-3	−120.50	−120.14	−124.37	−118.85
C-4	−121.50	−115.65	−118.29	−115.05
C-5	−119.89	−116.97	−115.41	−114.43
C-6[a]	−118.52	−115.93	−114.31	−113.59
C-7[a]	−116.00	−113.69	−111.94	−111.30

[a] The C-5-embedded models are used for single point energy calculations.

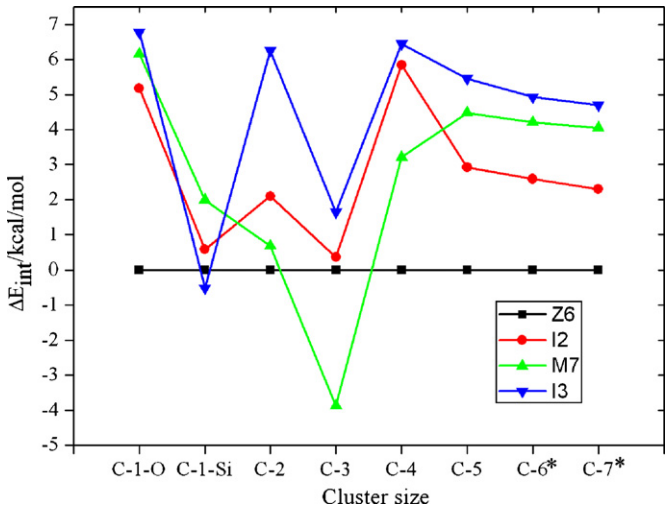

Fig. 6. Relative stabilities of Na-sites predicted by ΔE_{int}.

O–H and Si–H terminated cluster models in PA (proton affinity) calculations in H-ZSM-5 zeolite. They found that O–H termination caused unrealistically strong electrostatic potential on the terminal O–H groups, so O–H terminated models tended to overestimate PA for acid zeolite. We believe that the serious overestimation of E_{int}, observed here for C-1-O, is also due to the O–H termination. We suggest that other factors, such as the small size of C-1-O and the lack of the long-range interactions, also contribute. These effects can be inferred, as the calculated E_{int} further decrease gradually from C-1-Si to C-7.

Although the interaction energies do not converge at our largest C-7:192T cluster, what is actually important for the Na-site stability assessment is the relative interaction energies (ΔE_{int}) between different sites. From Table 4, we find that the differences between the calculated E_{int} with C-5 and C-6* models for Z6, I2, M7, I3 are 1.37, 1.04, 1.10 and 0.84 kcal/mol, respectively. On average, the calculated E_{int} with C-5 and C-6* clusters differ by 1.08 kcal/mol. However, the maximum deviation from this average value is only 0.29 kcal/mol. Thus both C-5 and C-6* predicted the same trend for ΔE_{int} as has shown in Table 3. Data in Table 4 show that the differences between the calculated E_{int} with C-6* and C-7* models for Z6, I2, M7 and I3 are 2.52, 2.24, 2.37 and 2.29 kcal/mol, respectively. The maximum deviation from the average value (2.36) is further reduced to 0.16 kcal/mol. We can conclude that further enlargement of the cluster size beyond C-5:75T will shift E_{int} for various Na-sites by similar amount, thus ΔE_{int} of different Na-sites start to converge at C-5 (see Fig. 6 and Section 3.4 for further discussion).

PA is usually used to characterize the acid strength of zeolites [81] which, in turn, is used as the indicator for the catalytic activity of acid zeolites. Brand et al. [80], used a series of cluster models ranging from 2T to 46T to calculate PA of H-ZSM-5. Similar to our results for E_{int} of the Na-sites, the calculated PAs changed with the increasing cluster size and no convergent results could be obtained within the cluster models they used. However, the present work showed that converged ΔE_{int} can be obtained with the C-5 type models, even though E_{int} does not converge. This suggests that ΔPA may also have a faster convergent behavior than PA itself. Indeed, we argue that it is ΔPA among different acid sites in zeolites that are more concerned with the elucidation of catalytic activity of the acid zeolites.

The cation localization energies (E_{loc}) of the Na-sites by various cluster models for all the four sites are summarized in Table 5. As is evident, the difference between E_{loc} from the smallest model (C-1-O) and the largest model (C-7*) is much smaller than the corresponding value of E_{int}, suggesting that E_{loc} has less size dependence than E_{int}. This may be explained as the latter involves E_{Al}^{-} which is the total energy of a negatively charged cluster. Nevertheless, we notice that, for cluster models below C-5, E_{loc} is still far from being convergent and ΔE_{loc} between different Na-sites changes acutely as the cluster size increases. Significantly, E_{loc} tends to converge by C-5 and further enlarging C-5 clusters to C-6, causes only little change in E_{loc} (0.39, 0.07, 0.12 and 0.14 kcal/mol for Z6, I2, M7 and I3, respectively). From C-6 to C-7, the differences of E_{loc} for Z6, I2, M7 and I3 further decrease to 0.25, 0.04, 0.09 and 0.02 kcal/mol, respectively. Hence converged E_{loc} can be obtained using the C-5 type models, which guarantee a converged ΔE_{loc} from C-5 up.

Table 5
Dependence of E_{loc} on cluster model selection (kcal/mol). All numbers have been shifted by adding 115.3 au.

Cluster size	Z6	I2	M7	I3
C-1-O	−21.23	−13.35	−24.80	−18.89
C-1-Si	−19.41	−11.62	−21.10	−12.72
C-2	−23.34	−17.76	−34.36	−18.86
C-3	−32.04	−27.73	−35.96	−26.44
C-4	−38.49	−32.64	−35.28	−32.03
C-5	−38.28	−35.36	−33.80	−32.82
C-6[a]	−37.88	−35.30	−33.67	−32.96
C-7[a]	−37.64	−35.34	−33.58	−32.94

[a] The C-5-embedded models are used for single point energy calculations.

Zygmunt et al. [82] calculated the activation barrier of ethane cracking on a series of cluster models of H-ZSM-5 with increasing size. They found that long-range interaction could largely stabilize the ionic transition state. E_{loc} is defined as the energy difference between the Al^{-}–Na^{+} and Si form clusters, where the ionic interaction plays an important role in stabilizing the Al^{-}–Na^{+} form clusters, which, in a way, is similar to the electronic structure for reaction with an ionic transition state. Indeed, the present work confirms this viewpoint as the calculated E_{loc} becomes more negative as the cluster size increases. Using models with a proper size (like C-5), the long-range electrostatic effect of the framework of zeolite is adequately accounted for, and converged results are thus achieved.

In ZSM-5, there are twelve distinct T-sites available [45]. The present work focuses on the Na^{+} location associated with the **T1** site. In the literature, energy change, similar to E_{loc} defined here, has been used to evaluate the relative stability of Al substitution at different **T** sites in zeolite [47,48]. Thus accurate E_{loc} values are valuable for reliable prediction of Al distribution. Former quantum chemical studies for this issue usually used small clusters [47]. However, from this work, it is clear that one has to take into account of the size dependence of E_{loc} and ΔE_{loc}. Currently, we are studying the thermodynamic stability of different **T** sites for Al substitution in ZSM-5. We anticipate that reliable results can be obtained with the C-5 type models.

3.4. Relative stability of different Na-sites

Figs. 6 and 7 display the relative stability of all four sites (Z6, M7, I2 and I3) predicted by ΔE_{int} and ΔE_{loc}, respectively. As can be seen, the results from small cluster model calculations are oscillating, and hence are not trustworthy. The source of errors is a combined result from the boundary effects, unreasonable electronic structures, the partial absence of the long-range interactions, etc. The calculated energies for different Na-sites start to converge only when the cluster size is increased up to C-5. This demonstrates that the zeolite lattice effect beyond C-5 is negligible on the stability prediction of the Na-sites. Furthermore, C-5 is proved to be much more efficient than C-6 and C-7 while maintaining accuracy. The time consumed by one step of self-consistent field calculation for C-5 Al–Na model

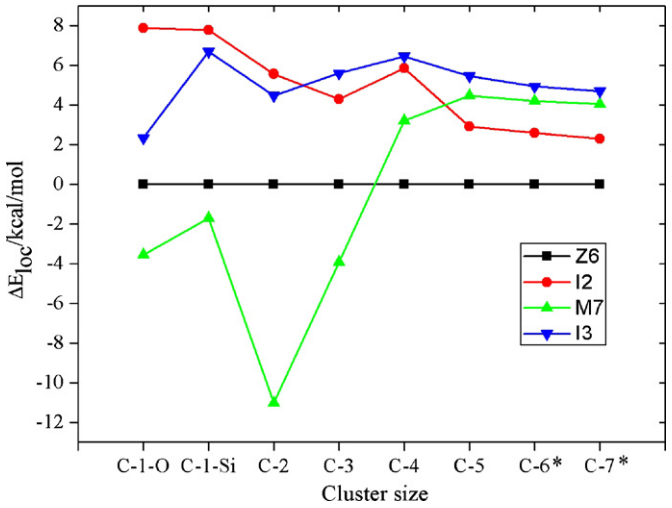

Fig. 7. Relative stabilities of Na-sites predicted by ΔE_{loc}.

of M7 is 2258s, while those for C-6 and C-7 are 4350s and 11,081s, respectively, on a dual processor Intel Xeon 5345–2.33 GHz Clovertown computer loaded with 8GB memory and 146GB disk space.

The final stability sequence of the four probable location sites for Na^+ at **T1** by the C-5 type clusters is Z6 > I2 > M7 > I3. The only result that is available to be compared with our work was provided by Kucera and Nachtigall [28]. They used an IPF (interatomic potential function) method to investigate the relative stability for Na^+ locating at M7, I2 (5-1-2) and another I2 (1-10-4) site, and found M7 and I2 (5-1-2) as the equally stable sites with E_{int} (E_b in Ref. [28]) to be −127 kcal/mol. Although Z6 is found to be the most stable site in our calculation, Z6 and I3 were not reported in their work, while our optimization could not locate a local minimum for I2 (1-10-4). Nachtigallova et al. [27] investigated Cu^+ location at **T1** site and found a Z6 site similar to that in this work. We have also tried to locate a Z5 site in which Na^+ located on top of a 5-member ring in the zigzag channel. Geometry optimizations using C-4, C-5 and C-6 cluster models in search for Z5 always end up with the I3 site. Hence, Z6, M7, I2 and I3 are the four probable sites that we can locate at the **T1** site.

The stability of a specific Na-site can be related to its local coordination environment. The Z6 site is predicted here to be the most stable site, as it possesses higher coordination numbers and higher geometric flexibility. The Z6 site can accommodate Na^+ well by a triple coordination with the corresponding Na–O bond lengths of 2.222, 2.334 and 2.478 Å, respectively. The Na–O bond lengths (2.262 Å and 2.347 Å) in I2 are comparable to those of Z6, but only two O atoms are available for Na^+ in this site. As compared to Z6, there is an additional SiO_4 at the bottom of the M7 site, which largely restricts its structural relaxation during Na^+ coordination to M7. In I3, three O atoms in AlO_4 are coordinated to Na^+. However the Na–O bonds are relatively longer (2.396, 2.412 and 2.483 Å). Significantly, the Al–Na distance in I3 site is fairly short (only 2.669 Å), while those in I2, M7 and Z6 are much longer (2.991, 3.020 and 3.479 Å, respectively). This leads to a larger repulsion between Na^+ and the positive-charged Al^{3+} in I3, which makes it the least favorable.

3.5. Proposed schemes for cluster model selection for cation location

There is no systematic study on the model selection for cation location in the literature. There are related works on the model selection for the Brønsted acid site in zeolites [80,83–85]. In these studies, a Si–O(H)–Al bridge structure was usually used as the center of the models and the full model was obtained by incorporating the environment around this central bridge. This scheme needs to be improved for metal cation location studies as the distribution of metal cations is much more flexible than H^+. In this work, the C-5 type model is found to be the smallest one with convergent coordination structure and stability sequence for all four Na-sites associated with **T1**. The key feature of C-5 is to allow all the atoms on the three rings around the Al site to relax during the geometry optimization, while expanding the region by roughly another three shells of Si atoms. In such a way, boundary effects are minimized and long range electrostatic interactions can be properly accounted for. We suggest that such a scheme can be applied to study cation location at other **T**-sites for Al substitutions. Encouraging preliminary results have been achieved and a more thorough study is in progress.

4. Conclusions

Here we present the first systematic investigation on the model selection in geometry optimization and relative stability prediction of the Na-sites associated with the **T1** site for Al substitution. The main conclusions are summarized as following:

1. Selection of the relaxed region during the partial geometry optimization has important impact on the optimized structures. Inclusion of long-range electrostatic interaction and elimination of cluster boundary effect are also important for reliable predictions of cation coordination geometry and cation stability sequence of various sites.
2. For Na-sites associated with the T1 site for Al substitution, we find that E_{loc} start to converge at the C-5:75T type models, while E_{int} is not yet converged even at C-7:192T. Both ΔE_{loc} and ΔE_{int} are converged at C-5, predicting a stability sequence of Z6 > I2 > M7 > I3.
3. The C-5 type model is constructed by allowing all the atoms on the three rings around the Al site to relax during the geometry optimization, and then expanding the region by roughly another three shells of Si atoms. We suggest that this is a general scheme to set up suitable cluster models for metal cation location calculations in zeolites.

Zeolites normally display a low symmetry with large unit cells due to the Si/Al substitution. This not only imposes technical difficulty in periodic method (e.g. The unit cell of ZSM-5 consists of 96T [45]), but also demands large cluster models for proper description (e.g. The C-5:75T model at 6-31G(d), recommended here, contains 259 atoms and 3331 basis functions). Hybrid methods (e.g. 'our own n-layered integrated molecular orbital and molecular mechanics' ONIOM method [34–37]) may present a promising alternative [38]. Our present work provides "the real values" for further ONIOM model study. Through proper selection of the high and low-level methods and high-layers in the ONIOM scheme, more efficient calculation schemes could be designed [34–38]. Further investigation on other **T** sites in ZSM-5 zeolite is needed for a comprehensive understanding of Na^+ location in this important high-silica zeolite.

Acknowledgements

This work was supported by the National Natural Science Foundation of China (10774126, 20923004), and the Ministry of Science and Technology (2007CB815206, 2011CB808505).

References

[1] R.A. van Santen, M. Neurock, Molecular Heterogeneous Catalysis, Wiley, Weinheim, 2006.

[2] A. Corma, H. Garcia, Chem. Rev. 102 (2002) 3837.
[3] C. Coperet, Chem. Rev. 110 (2010) 656.
[4] B. Wichterlova, Z. Sobalik, J. Dedecek, Appl. Catal. B: Environ. 41 (2003) 97.
[5] L.B. McCusker, C. Baerlocher, Stud. Surf. Sci. Catal. 168 (2007) 13.
[6] R.E. Morris, P.S. Wheatley, Stud. Surf. Sci. Catal. 168 (2007) 375.
[7] J. Dedecek, B. Wichterlova, J. Phys. Chem. B 103 (1999) 1462.
[8] D. Kaucky, J. Dedecek, B. Wichterlova, Micropor. Mesopor. Mater. 31 (1999) 75.
[9] J. Dedecek, D. Kaucky, B. Wichterlova, Micropor. Mesopor. Mater. 35–36 (2000) 483.
[10] J. Dedecek, L. Capek, D. Kaucky, Z. Sobalik, B. Wichterlova, J. Catal. 211 (2002) 198.
[11] Z. Sobalik, J. Dedecek, D. Kaucky, B. Wichterlova, L. Drozdova, R. Prins, J. Catal. 194 (2000) 330.
[12] L. Drozdova, R. Prins, J. Dedecek, Z. Sobalik, B. Wichterlova, J. Phys. Chem. B 106 (2002) 2240.
[13] S. Bordiga, E. Escalona Platero, C. Otero Arean, C. Lamberti, A. Zecchina, J. Catal. 137 (1992) 179.
[14] E. Garrone, B. Fubini, B. Bonelli, B. Onida, C. Otero Arean, Phys. Chem. Chem. Phys. 1 (1999) 513.
[15] B. Bonelli, E. Garrone, B. Fubini, B. Onida, M. Rodriguez Delgado, C. Otero Arean, Phys. Chem. Chem. Phys. 5 (2003) 2900.
[16] B. Bonelli, B. Fubini, B. Onida, G. Turnes Palomino, M. Rodriguez Delgado, C. Otero Arean, E. Garrone, Stud. Surf. Sci. Catal. 154 (2004) 1686.
[17] R.J. Accardi, R.F. Lobo, Micropor. Mesopor. Mater. 40 (2000) 25.
[18] M.Y. Kustova, S.B. Rasmussen, A.L. Kustov, C.H. Christensen, Appl. Catal. B: Environ. 67 (2006) 60.
[19] P. Decyk, Catal. Today 114 (2006) 142.
[20] A. Vinu, D.P. Sawant, K. Ariga, K.Z. Hossain, S.B. Halligudi, M. Hartmann, M. Nomura, Chem. Mater. 17 (2005) 5339.
[21] J.-H. Park, H.J. Park, J.H. Baik, I.-S. Nam, C.-H. Shin, J.-H. Lee, B.K. Cho, S.H. Oh, J. Catal. 240 (2006) 47.
[22] A.J. Maia, B. Louis, Y.L. Lam, M.M. Pereira, J. Catal. 269 (2010) 103.
[23] M. Høj, M.J. Beier, J.-D. Grunwaldt, S. Dahl, Appl. Catal. B: Environ. 93 (2009) 166.
[24] K. Shimizu, R. Maruyama, T. Hatamachi, T. Kodama, J. Phys. Chem. C 111 (2007) 6440.
[25] G.N. Vayssilov, M. Staufer, T. Belling, K.M. Neyman, H. Knozinger, N. Rosch, J. Phys. Chem. B 103 (1999) 7920.
[26] M.J. Rice, A.K. Chakraborty, A.T. Bell, J. Phys. Chem. B 104 (2000) 9987.
[27] D. Nachtigallova, P. Nachtigall, M. Sierka, J. Sauer, Phys. Chem. Chem. Phys. 1 (1999) 2019.
[28] J. Kucera, P. Nachtigall, Phys. Chem. Chem. Phys. 5 (2003) 3311.
[29] B. Civalleri, A.M. Ferrari, M. Llunell, R. Orlando, M. Merawa, P. Ugliengo, Chem. Mater. 15 (2003) 3996.
[30] L.A.M.M. Barbosa, R.A. van Santen, J. Phys. Chem. C 111 (2007) 8337.
[31] L. Benco, T. Bucko, R. Grybos, J. Hafner, Z. Sobalik, J. Dedecek, S. Sklenak, J. Hrusak, J. Phys. Chem. C 111 (2007) 9393.
[32] J. Sauer, Chem. Rev. 89 (1989) 199.
[33] P. Nachtigall, J. Sauer, Stud. Surf. Sci. Catal. 168 (2007) 701.
[34] S. Humbel, S. Sieber, K. Morokuma, J. Chem. Phys. 105 (1996) 1959.
[35] M. Svensson, S. Humbel, K. Morokuma, J. Chem. Phys. 105 (1996) 3654.
[36] S. Dapprich, I. Komaromi, K.S. Byun, K. Morokuma, M.J. Frisch, J. Mol. Struct.: Theochem. 461–462 (1999) 1.
[37] T. Vreven, K. Morokuma, J. Comput. Chem. 21 (2000) 1419.
[38] S.T. Bromley, C.R.A. Catlow, Th. Maschmeyer, Cattech 7 (2003) 164.
[39] C.S. Cundy, P.A. Cox, Chem. Rev. 103 (2003) 663.
[40] H. Hattori, Chem. Rev. 95 (1995) 537.
[41] D. Barthomeuf, Catal. Rev. Sci. Eng. 38 (1996) 521.
[42] S.V. Bordawekar, R.J. Davis, J. Catal. 189 (2000) 79.
[43] M. Sanchez-Sanchez, T. Blasco, J. Am. Chem. Soc. 124 (2002) 3443.
[44] P.M.M. Blauwhoff, J.W. Gosselink, E.P. Kieffer, S.T. Sie, W.H.J. Stork, Catalysis and zeolites—Fundamentals and Applications, Springer, Berlin, 1999.
[45] H. van Koningsveld, H. van Bekkum, J.C. Jansen, Acta Crystallogr. B43 (1987) 127.
[46] V.B. Kazansky, E.A. Pidko, Catal. Today 110 (2005) 281.
[47] A. Redondo, P.J. Hay, J. Phys. Chem. 97 (1993) 11754.
[48] G. Ricchiardi, J.M. Newsam, J. Phys. Chem. B 101 (1997) 9943.
[49] J.C. Slater, The Self-consistent Field for Molecules and Solids; In Quantum Theory of Molecules and Solids, Mc-Graw Hill, New York, 1974.
[50] S.H. Vosko, L. Wilk, M. Nusair, Can. J. Psychiatry 58 (1980) 1200.
[51] A.D. Becke, Phys. Rev. A 38 (1988) 3098.
[52] A.D. Becke, J. Chem. Phys. 98 (1993) 5648.
[53] C.T. Lee, W.T. Yang, R.G. Parr, Phys. Rev. B 37 (1988) 785.
[54] J.S. Binkley, J.A. Pople, W.J. Hehre, J. Am. Chem. Soc. 102 (1980) 939.
[55] M.S. Gordon, J.S. Binkley, J.A. Pople, W.J. Pietro, W.J. Hehre, J. Am. Chem. Soc. 104 (1982) 2797.
[56] W.J. Pietro, M.M. Francl, W.J. Hehre, D.J. Defrees, J.A. Pople, J.S. Binkely, J. Am. Chem. Soc. 104 (1982) 5039.
[57] K.D. Dobbs, W.J. Hehre, J. Comput. Chem. 7 (1986) 359.
[58] K.D. Dobbs, W.J. Hehre, J. Comput. Chem. 8 (1987) 861.
[59] K.D. Dobbs, W.J. Hehre, J. Comput. Chem. 8 (1987) 880.
[60] M.S. Gordon, Chem. Phys. Lett. 76 (1980) 163.
[61] M.M. Francl, W.J. Pietro, W.J. Hehre, J.S. Binkley, M.S. Gordon, D.J. Defrees, J.A. Pople, J. Chem. Phys. 77 (1982) 3654.
[62] P.C. Hariharan, J.A. Pople, Theor. Chim. Acta (Berl.) 28 (1973) 213.
[63] G.A. Peterson, A. Bennett, T.G. Tensfeldt, M.A. Al-Laham, W.A. Shirley, J. Mantzairis, J. Chem. Phys. 89 (1988) 2193.
[64] M.A. Al-Laham, G.A. Petersson, J. Chem. Phys. 94 (1991) 6081.
[65] A.D. McLean, G.S. Chandler, J. Chem. Phys. 72 (1980) 5639.
[66] R. Krishnan, J.S. Binkley, R. Seeger, J.A. Pople, J. Chem. Phys. 72 (1980) 650.
[67] R.C. Binning Jr, L.A. Curtiss, J. Comput. Chem. 11 (1990) 1206.
[68] L.A. Curtiss, M.P. McGrath, J.P. Blaudeau, N.E. Davis, R.C. Binning Jr, L. Radom, J. Chem. Phys. 103 (1995) 6104.
[69] M.P. McGrath, L. Radom, J. Chem. Phys. 94 (1991) 511.
[70] M.J. Frisch, G.W. Trucks, H.B. Schlegel, G.E. Scuseria, M.A. Robb, J.R. Cheeseman, J.A. Montgomery Jr, T. Vreven, K.N. Kudin, J.C. Burant, J.M. Millam, S.S. Iyengar, J. Tomasi, V. Barone, B. Mennucci, M. Cossi, G. Scalmani, N. Rega, G.A. Petersson, H. Nakatsuji, M. Hada, M. Ehara, K. Toyota, R. Fukuda, J. Hasegawa, M. Ishida, T. Nakajima, Y. Honda, O. Kitao, H. Nakai, M. Klene, X. Li, J.E. Knox, H.P. Hratchian, J.B. Cross, V. Bakken, C. Adamo, J. Jaramillo, R. Gomperts, R.E. Stratmann, O. Yazyev, A.J. Austin, R. Cammi, C. Pomelli, J.W. Ochterski, P.Y. Ayala, K. Morokuma, G.A. Voth, P. Salvador, J.J. Dannenberg, V.G. Zakrzewski, S. Dapprich, A.D. Daniels, M.C. Strain, O. Farkas, D.K. Malick, A.D. Rabuck, K. Raghavachari, J.B. Foresman, J.V. Ortiz, Q. Cui, A.G. Baboul, S. Clifford, J. Cioslowski, B.B. Stefanov, G. Liu, A. Liashenko, P. Piskorz, I. Komaromi, R.L. Martin, D.J. Fox, T. Keith, M.A. Al-Laham, C.Y. Peng, A. Nanayakkara, M. Challacombe, P.M.W. Gill, B. Johnson, W. Chen, M.W. Wong, C. Gonzalez, J.A. Pople, Gaussian 03, Revision D.01, Gaussian, Inc., Wallingford, CT, 2004.
[71] T. Verstraelen, D. Van Neck, P.W. Ayers, V. Van Speybroeck, M. Waroquier, J. Chem. Theory Comput. 3 (2007) 1420.
[72] O. Saengsawang, T. Remsungnen, S. Fritzsche, R. Haberlandt, S. Hannongbua, J. Phys. Chem. B 109 (2005) 5684.
[73] X. Zheng, P. Blowers, J. Phys. Chem. A 109 (2005) 10734.
[74] A. Itadani, H. Sugiyama, M. Tanaka, T. Ohkubo, T. Yumura, H. Kobayashi, Y. Kuroda, J. Phys. Chem. C 113 (2009) 7213.
[75] E. Kassab, M. Castella-Ventura, Y. Akacem, J. Phys. Chem. C 113 (2009) 20388.
[76] J. Sauer, Cluster Models for Surface and Bulk Phenomena, Plenum Press, New York, 1992.
[77] M. Boronat, C.M. Zicovich-Wilson, P. Viruela, A. Corma, Chem. Eur. J. 7 (2001) 1295.
[78] J.T. Fermann, T. Moniz, O. Kiowski, T.J. McIntire, S.M. Auerbach, T. Vreven, M.J. Frisch, J. Chem. Theory Comput. 1 (2005) 1232.
[79] R.W. Joyner, A.D. Smith, M. Stockenhuber, M.W.E. van Den Berg, Stud. Surf. Sci. Catal. 154 (2004) 1406.
[80] H.V. Brand, L.A. Curtiss, L.E. Iton, J. Phys. Chem. 97 (1993) 12773.
[81] R.A. van Santen, G.J. Kramer, Chem. Rev. 95 (1995) 637.
[82] S.A. Zygmunt, L.A. Curtiss, P. Zapol, L.E. Iton, J. Phys. Chem. B 104 (2000) 1944.
[83] H.V. Brand, L.A. Curtiss, L.E. Iton, J. Phys. Chem. 96 (1992) 7725.
[84] U. Eichler, M. Brandle, J. Sauer, J. Phys. Chem. B 101 (1997) 10035.
[85] K. Sillar, P. Burk, J. Phys. Chem. B 108 (2004) 9893.